Journal of Mathematical Biology (2022) 85:10
https://doi.org/10.1007/s00285-022-01767-7

Mathematical Biology

How influenza vaccination and virus interference may impact combined influenza-coronavirus disease burden

Mohammed H. Alharbi[1] · Christopher M. Kribs[2]

Received: 26 April 2021 / Revised: 14 May 2022 / Accepted: 2 June 2022 /
Published online: 15 July 2022

Abstract
Demand for influenza vaccine rose as countries prepared for the second COVID-19 wave over the winter months of 2020-2021. High coverage of the influenza vaccine can significantly reduce morbidity and mortality of the burden of influenza. Natural influenza infection creates short-term non-specific immunity against respiratory viruses (virus interference). We model two viral diseases, both of the SEIR type, to investigate whether the influenza vaccine increases the combined disease burden of influenza and COVID-19 in a dual outbreak. We show that the combined disease burden's behavior depends on virus interference factors and the proportion of the population vaccinated against influenza. Our results indicate that influenza vaccination only lowers the overall disease burden when net virus interference is relatively low.

Mathematics Subject Classification 92D30 · 92B99

1 Introduction

The current pandemic of coronavirus disease 2019 (COVID-19) is caused by infection with a new coronavirus (called SARS-CoV-2). Influenza (flu) is a contagious respiratory disease caused by influenza viruses. Both diseases are infectious respiratory illnesses. There are some critical differences between flu and COVID-19. COVID-19 differs from influenza in the mortality rate, infectiousness by individuals with no symptoms, and spreading more quickly. While there has long been a vaccine to protect against influenza, vaccines for COVID-19 are just beginning to be distributed around the world.

✉ Mohammed H. Alharbi
mhhalharbi1@uj.edu.sa

[1] Department of Mathematics, College of Science, University of Jeddah, Jeddah, Saudi Arabia

[2] Department of Mathematics, University of Texas at Arlington, Arlington, TX 76019, USA

Even though the influenza vaccine gives no protection against COVID-19 (Shahid et al. 2020), demand for influenza vaccine rose as countries planned for the second COVID-19 wave over the winter months of 2020-2021. High coverage of the vaccine can significantly reduce morbidity and mortality of the burden of influenza.

Although the influenza vaccine may protect against the risk of influenza, natural influenza infection may reduce the risk of noninfluenza respiratory viruses (NRV) by activating short-term non-specific immunity against these viruses, a phenomenon known as virus interference. In other words, individuals who have received the influenza vaccine may be at higher risk for NRV infections than individuals who have had influenza infections because they do not exhibit the non-specific immunity associated with natural infection (Feng et al. 2017; Suzuki et al. 2014; Cowling and Nishiura 2012; Cowling et al. 2012; Kelly et al. 2010). Studies in children and adults support the idea that the influenza vaccine may increase the risk of NRV infections compared to individuals recently recovered from influenza. A recent Dutch study among older adults showed an increased incidence of NRV infections in vaccinated versus unvaccinated persons (Van Beek et al. 2017). A study in children who received the influenza vaccine reported four times more NRV infections (Cowling et al. 2012). In the case of adults, one study found a 36% increase in risk related to coronavirus infections (Wolff 2020).

It is still not clear whether COVID-19 infection causes similar interference with influenza or other respiratory viruses. Further, there is no definitive evidence about whether the influenza vaccine prevents virus interference with COVID-19. Limited knowledge has been available regarding whether the influenza vaccine affects COVID-19 infection risk. There are conflicting studies concerning this aspect. While some studies found that the influenza vaccination coverage rates correlated negatively with all COVID-19 outcomes (Amato et al. 2020; Martínez-Baz et al. 2020), other studies found that influenza vaccination coverage rates are associated significantly with recently observed COVID-19 infection rates (Lisewski 2020; EBMPHET Consortium 2020).

Ozaras et al. demonstrated that COVID-19 and influenza co-infection is rare. During their study period, 1103 patients were diagnosed with COVID-19. Among them, six patients (0.54%) were diagnosed co-infected with influenza (Ozaras et al. 2020). Ding et al. confirmed that few patients were co-infected by both diseases. A total of 5 of the 115 patients confirmed with COVID-19 were also diagnosed with influenza virus infection, with three influenza A cases and two influenza B (Ding et al. 2020).

Mathematical models have been developed to improve our knowledge of respiratory virus transmission and study different aspects of viral interference dynamics, such as influenza-influenza interactions and influenza-NRV interactions. Despite the mounting evidence of influenza and NRV interactions, mathematical models on influenza and NRV interference are rare (Opatowski et al. 2018). A recent study by Velasco-Hernández et al. explained the interaction observed between influenza and respiratory syncytial virus (RSV) by using an SEIRS model and provided some evidence that RSV dominates influenza. Their model is a superinfection model where RSV infection takes over influenza infection. Furthermore, in their model, individuals already infected with influenza are less susceptible to RSV infection than healthy individuals because the authors assume that infected individuals will be taking some precautionary

measures (Velasco-Hernández et al. 2015). Merler et al. used a mathematical model to illustrate the role of acute respiratory infections in the transmission dynamics of the 1918 influenza pandemic. The authors proposed that co-infection with other respiratory pathogens leads to enhanced influenza transmission. Their model produced results that agree with mortality excess data during 1918 pandemic influenza (Merler et al. 2008). None of these studies have to do with the virus interference phenomenon and vaccination. There is no mathematical study that incorporates both virus interference and influenza vaccine to the best of our knowledge.

This study aims to evaluate whether the influenza vaccine increases the combined disease burden of influenza and COVID-19 in a dual outbreak by using a mathematical compartmental model with differential equations. In this study, the well-known concept of DALY (Disability-Adjusted Life Years) is used to measure the combined disease burden. This calculation has two components for each disease: DALY for the survivals and DALY for non-survivals. We use dynamical systems models as tools to compare the outcomes of the influenza vaccine on the population.

2 Model development

The model is developed to analyze respiratory infection, in which we consider two distinct diseases; disease 1 indicates influenza, and disease 2 indicates COVID-19.

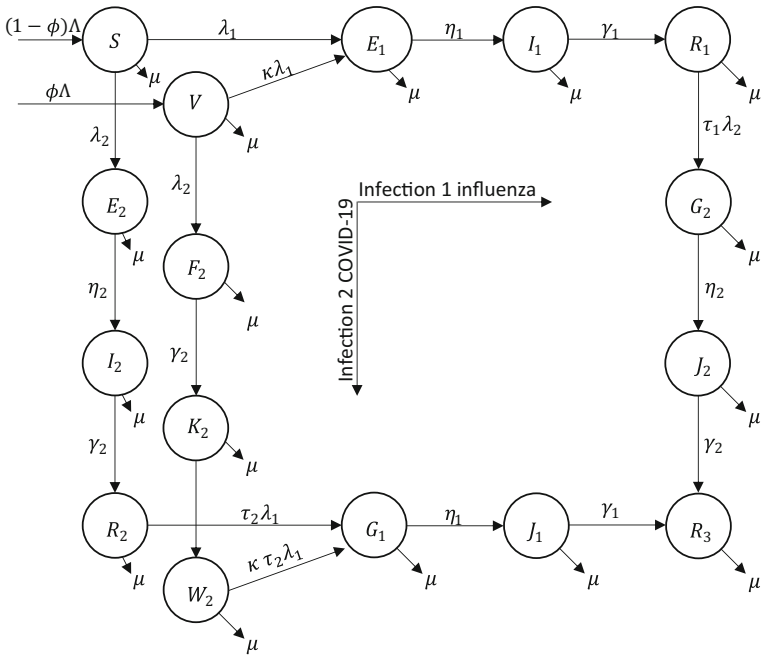

Fig. 1 Flowchart of model (1), where $\lambda_1 = \beta_1 \frac{I_1+J_1}{N}$ and $\lambda_2 = \beta_2 \frac{I_2+J_2+K_2}{N}$

We divide the total population into susceptible (S), vaccinated (V), exposed (E_1 and E_2), infected (I_1 and I_2), and recovered (R_1 and R_2) compartments for each disease. Those vaccinated individuals infected by COVID-19 retain partial protection against influenza, requiring a separate chain of exposed (F_2), infective (K_2), and recovered (W_2) compartments. Individuals who recovered from disease 1 or 2 remain susceptible to the other disease, also requiring a separate chain of exposed (G_1 and G_2) and infective (J_1 and J_2) for each disease and recovered (R_3) compartments. Susceptible and vaccinated individuals can be infected by disease 1 (with a reduced rate for vaccinated individuals because of the vaccine's protection) through their contact with infected individuals in classes I_1 and J_1, or by disease 2 through their contact with infected individuals in classes I_2, K_2 and J_2 (with no vaccine protection). Following the observation that co-infection is rare, we assume that no one acquires a secondary infection during a primary infection. The model is described as follows:

$$
\begin{cases}
\frac{dS}{dt} = (1-\phi)\Lambda - \left[\beta_1 \frac{I_1+J_1}{N} + \beta_2 \frac{I_2+J_2+K_2}{N} + \mu\right] S, \\
\frac{dV}{dt} = \phi\Lambda - \left[\kappa\beta_1 \frac{I_1+J_1}{N} + \beta_2 \frac{I_2+J_2+K_2}{N} + \mu\right] V, \\
\frac{dE_1}{dt} = \beta_1 \frac{I_1+J_1}{N} S + \kappa\beta_1 \frac{I_1+J_1}{N} V - (\eta_1+\mu)E_1, \\
\frac{dE_2}{dt} = \beta_2 \frac{I_2+J_2+K_2}{N} S - (\eta_2+\mu)E_2, \\
\frac{dF_2}{dt} = \beta_2 \frac{I_2+J_2+K_2}{N} V - (\eta_2+\mu)F_2, \\
\frac{dI_1}{dt} = \eta_1 E_1 - (\gamma_1+\mu)I_1, \\
\frac{dI_2}{dt} = \eta_2 E_2 - (\gamma_2+\mu)I_2, \\
\frac{dK_2}{dt} = \eta_2 F_2 - (\gamma_2+\mu)K_2, , \\
\frac{dR_1}{dt} = \gamma_1 I_1 - \mu R_1 - \tau_1\beta_2 \frac{I_2+J_2+K_2}{N} R_1, \\
\frac{dR_2}{dt} = \gamma_2 I_2 - \mu R_2 - \tau_2\beta_1 \frac{I_1+J_1}{N} R_2, \\
\frac{dW_2}{dt} = \gamma_2 K_2 - \mu W_2 - \kappa\tau_2\beta_1 \frac{I_1+J_1}{N} W_2, \\
\frac{dG_1}{dt} = \tau_2\beta_1 \frac{I_1+J_1}{N} R_2 + \kappa\tau_2\beta_1 \frac{I_1+J_1}{N} W_2 - (\eta_1+\mu)G_1, \\
\frac{dG_2}{dt} = \tau_1\beta_2 \frac{I_2+J_2+K_2}{N} R_1 - (\eta_2+\mu)G_2, \\
\frac{dJ_1}{dt} = \eta_1 G_1 - (\gamma_1+\mu)J_1, \\
\frac{dJ_2}{dt} = \eta_2 G_2 - (\gamma_2+\mu)J_2, \\
\frac{dR_3}{dt} = \gamma_1 J_1 + \gamma_2 J_2 - \mu R_3,
\end{cases}
\tag{1}
$$

where β_1 and β_2 are influenza and COVID-19 infection rates, respectively. These infections are spreading in a large population; therefore, we assume that the contact rates are already saturated. Hence, we use standard incidence in this model instead of mass action. κ is the reduced susceptibility factor due to influenza vaccine protection, a dimensionless value between zero and one. Here η_1 and η_2 are the rates at which an individual departs exposed classes by becoming infectious. γ_1 and γ_2 are the recovery rates of influenza and COVID-19, respectively (Fig. 1).

Table 1 State variable and parameter definitions and their units

	Notation	Definition
State variables	$S(t)$	Number of susceptible individuals at time t
	$V(t)$	Number of individuals who have received the influenza vaccine at time t
	$E_i(t)$	Number of individuals who have been exposed to disease i at time t
	$I_i(t)$	Number of individuals who have been infected by disease i at time t
	$F_2(t)$	Number of individuals who have received the influenza vaccine and exposed to disease 2 at time t
	$K_2(t)$	Number of individuals who have received the influenza vaccine and infected by disease 2 at time t
	$R_i(t)$	Number of individuals who have recovered from disease i at time t
	$W_2(t)$	Number of individuals who have received the influenza vaccine and recovered from disease 2 at time t
	$G_i(t)$	Number of individuals who have been exposed to disease i and immunized by the other disease due to recovery at time t
	$J_i(t)$	Number of individuals who have been infected by disease i and immunized by the other disease due to recovery at time t
	$R_3(t)$	Number of individuals who have recovered from both diseases at time t
Parameters	Λ	Recruitment rate (Individual/Time)
	μ	Per capita natural mortality rate (1/Time)
	β_i	disease i infection rate (1/Time)
	ϕ	The proportion of individuals who have received the flu vaccine (Dimensionless)
	κ	Reduced susceptibility factor due to the flu vaccine protection (Dimensionless)
	η_i	1/The duration time from exposure to onset of infectivity for disease i (1/Time)
	γ_i	Disease i recovery rate (1/Time)
	τ_i	Virus interference reduced rate after recovery from disease i (Dimensionless)

We consider that individuals who recover from disease 1 or 2 (R_1 or R_2) will be less susceptible to the other disease due to virus interference. We incorporate the phenomenon of virus interference as parameters τ_1 and τ_2 that can tune between 0 and 1. τ_1 (τ_2) is the factor by which individuals who have recovered from disease 1 (disease 2) are less susceptible to a disease 2 (disease 1) infection (Table 1).

By adding Eq. (1), we get

$$\frac{dN}{dt} = \Lambda - \mu N$$

and

$$N(t) = \frac{\Lambda}{\mu} + e^{-\mu t}\left(N_0 - \frac{\Lambda}{\mu}\right),$$

where N_0 is the initial total population of the system. Then, taking the limit as $t \to \infty$:

$$\lim_{t\to\infty} N(t) = \frac{\Lambda}{\mu}.$$

Since we are aiming at a constant population and not interested in the demographic growth in this study, we assume that N is a constant population by taking $N(0) = \frac{\Lambda}{\mu}$. Therefore, the total population is constant for all t.

In this study, we have two additional differential equations to calculate the cumulative number of infections of disease 1, $C_1(t)$, and disease 2, $C_2(t)$

$$\begin{aligned}
\frac{dC_1}{dt} &= \beta_1 \frac{I_1 + J_1}{N} S + \kappa\beta_1 \frac{I_1 + J_1}{N} V + \tau_2\beta_1 \frac{I_1 + J_1}{N} R_2 + \kappa\tau_2\beta_1 \frac{I_1 + J_1}{N} W_2, \\
\frac{dC_2}{dt} &= \beta_2 \frac{I_2 + J_2 + K_2}{N} S + \beta_2 \frac{I_2 + J_2 + K_2}{N} V + \tau_1\beta_2 \frac{I_2 + J_2 + K_2}{N} R_1.
\end{aligned}$$

The combined disease burden can be estimated by using a cost function determined by the cumulative number of infections and the total number of deaths for each disease. The cost function determines the number of Disability Adjusted Life Years (DALY), which can be considered a loss of healthy life. The DALY is formed of Years of Life lived with Disability (YLD), resulting from infections, and Years of Life Lost (YLL) caused by death (Murray 1994). To estimate DALY components, we have

$$YLD_i = (1 - d_i) C_i(t) DW_i \frac{1}{\gamma_i},$$

where d_i is the case fatality ratio for disease i, $C_i(t)$ is the cumulative number of infections for disease i at time t, $\frac{1}{\gamma_i}$ is the average duration (in years) of infection for disease i, and DW_i is the disease weight. The term DW_i is assumed to be one for each disease. Further, we have

$$YLL_i = d_i C_i(t) L_i,$$

where L_i is the standard life expectancy at the age of death for disease i (average life expectancy at birth − average age of infection). Therefore, for each disease i we have

$$\begin{aligned}
DALY_i &= YLD_i + YLL_i \\
&= (1 - d_i) C_i(t) DW_i \frac{1}{\gamma_i} + d_i C_i(t) L_i \\
&= C_i(t)[(1 - d_i) DW_i \frac{1}{\gamma_i} + d_i L_i].
\end{aligned}$$

Then, finally the combined disease burden cost function is

$$DB(t) = C_1(t)\left[(1 - d_1) DW_1 \frac{1}{\gamma_1} + d_1 L_1\right] + C_2(t)\left[(1 - d_2) DW_2 \frac{1}{\gamma_2} + d_2 L_2\right].$$

3 Analysis

3.1 Disease free equilibrium and control reproductive numbers

In this section, we compute the control reproductive number (CRN) which is one of the most significant thresholds that measures the infection's ability to spread. We use $\mathcal{R}_c$ instead of using the basic reproduction number, $\mathcal{R}_0$, because it includes vaccination as a control measure. In order to derive the $\mathcal{R}_c$ for model (1), we perform an equilibrium analysis.

The disease-free equilibrium (DFE) is a point where no disease is present in the population and occurs for model (1) when $I_i^* = J_i^* = K_2^* = 0$ for all $i = 1, 2$. By setting all differential equations in (1) equal to zero, we find the DFE of the form $\frac{\Lambda}{\mu}((1-\phi), \phi, 0, 0, 0, 0, 0, 0, 0, 0, 0, 0, 0, 0, 0, 0)$.

To determine under what conditions infection with disease 1 or disease 2 can persist in the population, we determine the control reproductive numbers for each infection. The control reproductive number is a threshold condition defined to be the average number of secondary infections caused by one primary infected individual in a wholly uninfected population under a control strategy. We compute $\mathcal{R}_1$ for disease 1, $\mathcal{R}_2$ for disease 2, and $\mathcal{R}_c$ for the presence of any infection with either disease.

To drive the various reproductive numbers of the diseases in the model, we use the next-generation operator method (Van den Driessche and Watmough 2002). We find $\mathcal{R}_c = \max\{\mathcal{R}_1, \mathcal{R}_2\}$ where

$$\mathcal{R}_1 = \frac{\eta_1}{\eta_1 + \mu}\frac{\beta_1}{\gamma_1 + \mu}\left[(1-\phi) + \kappa\phi\right], \quad \mathcal{R}_2 = \frac{\eta_2}{\eta_2 + \mu}\frac{\beta_2}{\gamma_2 + \mu}.$$

The first two parts of $\mathcal{R}_1$ and $\mathcal{R}_2$ can be interpreted as the following. The first fraction $(\frac{\eta_i}{\eta_i+\mu})$ is the proportion of exposed individuals who did not die before they progress to infectious status. The second fraction $(\frac{\beta_i}{\gamma_i+\mu})$ is the product of the disease i infection rate and the average time an individual remains infected with disease i. The additional part of $\mathcal{R}_1$ is the proportion of vaccinated individuals (ϕ) times the reduced susceptibility factor (κ) due to the vaccine effectiveness added to the proportion of individuals who have not received the vaccine $(1-\phi)$.

We see that reduced infection factors of recovered individuals due to virus interference (τ_1 and τ_2) do not appear in the CRN because each of them occurs when the other infection is persistent. In an initial outbreak scenario, neither infection would be persisting in the population. Therefore, τ_1 and τ_2 should not be expected to appear in the CRN, but in the invasion reproductive numbers (IRNs).

3.2 Endemic equilibria and invasion reproductive numbers

We find another equilibrium when there is no infection with disease 2. In this case, $I_2^* = K_2^* = J_2^* = 0$. By setting all the nonlinear differential equations in model (1) equations equal to zero, we get $E_2^* = F_2^* = G_2^* =$

$W_2^* = R_2^* = G_1^* = J_1^* = R_3^* = 0$ and the equilibrium is $EE_1 = \frac{\Lambda}{\mu}(\frac{1-\phi}{1+m}, \frac{\phi}{1+\kappa m}, \frac{(\gamma_1+\mu)m\mu}{\eta_1\beta_1}, 0, 0, \frac{m\mu}{\beta_1}, 0, 0, \frac{\gamma_1 m}{\beta_1}, 0, 0, 0, 0, 0, 0, 0)$, where

$$m = \frac{\kappa(\mathcal{R}_1 - 1) - (1 - (1-\kappa^2)\phi) + \sqrt{((1-(1-\kappa^2)\phi) - \kappa(\mathcal{R}_1 - 1))^2 + 4\kappa(1-(1-\kappa)\phi)(\mathcal{R}_1 - 1)}}{2\kappa(1-(1-\kappa)\phi)}.$$

Observe that this equilibrium makes biological sense only when $\mathcal{R}_1 > 1$. Further, the sum of uninfected compartments at EE_1 is $\frac{1+m(\kappa(1-\phi)+\phi)}{(1+m)(1+\kappa m)}$ and infected compartments is $\frac{m(1-(1-\kappa)\phi)}{\mathcal{R}_1}$.

The second single-disease equilibrium is found when there is no infection with disease 1. In this case, $I_1^* = J_1^* = 0$. By setting all differential equations in model 1 equal zero, we get $E_1^* = G_1^* = R_1^* = G_2^* = J_2^* = R_3^* = 0$ and and the equilibrium is $EE_2 = \frac{\Lambda}{\mu}(\frac{1-\phi}{\mathcal{R}_2}, \frac{\phi}{\mathcal{R}_2}, 0, \frac{(\mathcal{R}_2-1)(1-\phi)(\gamma_2+\mu)\mu}{\beta_2\eta_2}, \frac{(\mathcal{R}_2-1)\phi(\gamma_2+\mu)\mu}{\beta_2\eta_2}, 0, \frac{(\mathcal{R}_2-1)(1-\phi)\mu}{\beta_2}, \frac{(\mathcal{R}_2-1)\phi(\gamma_2+\mu)\mu}{\beta_2}, 0, \frac{(\mathcal{R}_2-1)(1-\phi)\gamma_2}{\beta_2}, \frac{(\mathcal{R}_2-1)\phi\gamma_2}{\beta_2}, 0, 0, 0, 0, 0)$.

We observe that the total population at EE_2 is $\frac{\Lambda}{\mu}$ (the sum of uninfected compartments is $\frac{1}{\mathcal{R}_2}$ and infected compartments is $1 - \frac{1}{\mathcal{R}_2}$) . Further, this equilibrium makes biological sense only when $\mathcal{R}_2 > 1$.

The invasion reproductive number (IRN), which is defined to be the average number of secondary infections caused by one primary infected individual with one disease in an environment where the other disease is endemic, measures the ability of a disease to invade while another disease is present and at equilibrium (Mitchell and Kribs 2019; Kribs-Zaleta and Mubayi 2012; Zhang et al. 2007; Porco and Blower 1998).

We define IRN $\tilde{\mathcal{R}}_1$ to be the average number of secondary disease 1 infections caused by an infected individual introduced into a population at EE_2. $\tilde{\mathcal{R}}_2$ is defined similarly.

$\tilde{\mathcal{R}}_1$ is found through the next-generation operator method at EE_2, where we calculate the spectral radius of the matrix $F_1 V_1^{-1}$ (Van den Driessche and Watmough 2002). In this method, we assume implicitly that $\mathcal{R}_2 > 1$. We compute the spectral radius of $F_1 V_1^{-1}$ is given by

$$\tilde{\mathcal{R}}_1 = \mathcal{R}_1 \left[\frac{1}{\mathcal{R}_2} + \tau_2 \left(\frac{\gamma_2}{\gamma_2 + \mu} \frac{\eta_2}{\eta_2 + \mu} \right) \left(1 - \frac{1}{\mathcal{R}_2} \right) \right].$$

We observe that $\tilde{\mathcal{R}}_1$ is essentially $\mathcal{R}_1$ multiplied by a term representing a weighted average susceptibility to infection: the uninfected proportion at EE_2 ($\frac{1}{\mathcal{R}_2}$) weighting relative (unchanged) susceptibility 1, and the infected proportion ($1 - \frac{1}{\mathcal{R}_2}$) weighting their average susceptibility τ_2 multiplied by the proportion of infecteds who do not die while infected (since by assumption the infected are unavailable for infection until they recover).

We also consider the IRN $\tilde{\mathcal{R}}_2$. $\tilde{\mathcal{R}}_2$ represents the ability of disease 2 to invade a susceptible population at EE_1. $\tilde{\mathcal{R}}_2$ is found similar to $\tilde{\mathcal{R}}_1$ and given by

$$\tilde{\mathcal{R}}_2 = \mathcal{R}_2 \left[\left(\frac{1 + m(\kappa(1-\phi) + \phi)}{(1+m)(1+\kappa m)} \right) + \tau_1 \left(\frac{\gamma_1}{\gamma_1 + \mu} \frac{\eta_1}{\eta_1 + \mu} \right) \left(\frac{m(1-(1-\kappa)\phi)}{\mathcal{R}_1} \right) \right].$$

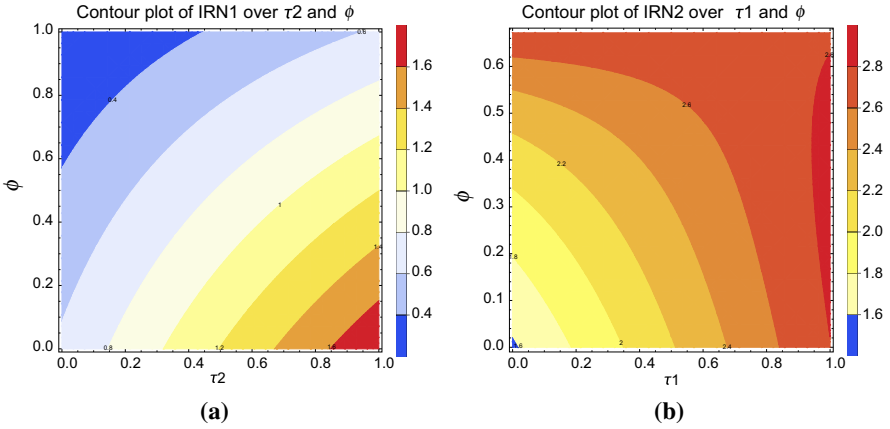

(a) **(b)**

Fig. 2 Contour plot of IRN1 (IRN2) over ϕ and τ_2 and (τ_1)

$\tilde{\mathcal{R}}_2$ can be interpreted term by term similarly to those for $\tilde{\mathcal{R}}_1$. From this view, we can see that $\tilde{\mathcal{R}}_2$ is $\mathcal{R}_2$ multiplied by a weighted average susceptibility to infection: the uninfected proportion at EE_1 ($\frac{1+m(\kappa(1-\phi)+\phi)}{(1+m)(1+\kappa m)}$) weighting relative (unchanged) susceptibility 1, and the infected proportion ($\frac{m(1-(1-\kappa)\phi)}{\mathcal{R}_1}$) weighting their average susceptibility τ_1 multiplied by the proportion of infecteds who do not die while infected.

4 Numerical simulations

To address this study's goal, we take parameter values directly from Alharbi and Kribs (2021, 2022). We consider disease 1 to be influenza H3N2 and disease 2 is COVID-19. Further, we allow the proportion of individuals who have received the vaccine (ϕ) to vary between 0 and 1 as a control measure.

For the estimation of parameter values of our cost function, we have the average age of the infection of influenza in the U.S. as 32.36 (CDC 2020) and COVID-19 as 41.1 (CDC 2021), and the average life expectancy at birth for the total U.S. population as 77.8 years (U.S. Census Bureau 2019). That gives $L_1 = 77.8 - 32.36 = 45.44$ and $L_2 = 77.8 - 41.1 = 36.7$. We estimate case fatality ratios for influenza and COVID-19 by calculating the case fatality ratio for each age group from CDC (2020, 2021) and then multiplying each age group's case fatality ratio by the proportion of the whole population in that age group, and summing the results (U.S. Census Bureau 2019), which gives $d_1 = 0.031\%$ and $d_2 = 1.96\%$. All these parameters give us an estimate of 0.02 DALY for one average case of influenza and 0.73 DALY for one average case of COVID-19.

Figure 2(a) (Fig. 2(b)) is a contour plot of $\tilde{\mathcal{R}}_1$ ($\tilde{\mathcal{R}}_2$) over τ_2 (τ_1) and ϕ. First, for Fig. 2(a), we observed that $\tilde{\mathcal{R}}_1$ increases with τ_2, which indicates that virus interference plays a major role in reducing $\tilde{\mathcal{R}}_1$. Besides, $\tilde{\mathcal{R}}_1$ decreases with ϕ, indicating that as the proportion of individuals who received the influenza vaccine increased, the ability of influenza to spread becomes difficult. Then, for Fig. 2(b), we observed that $\tilde{\mathcal{R}}_2$

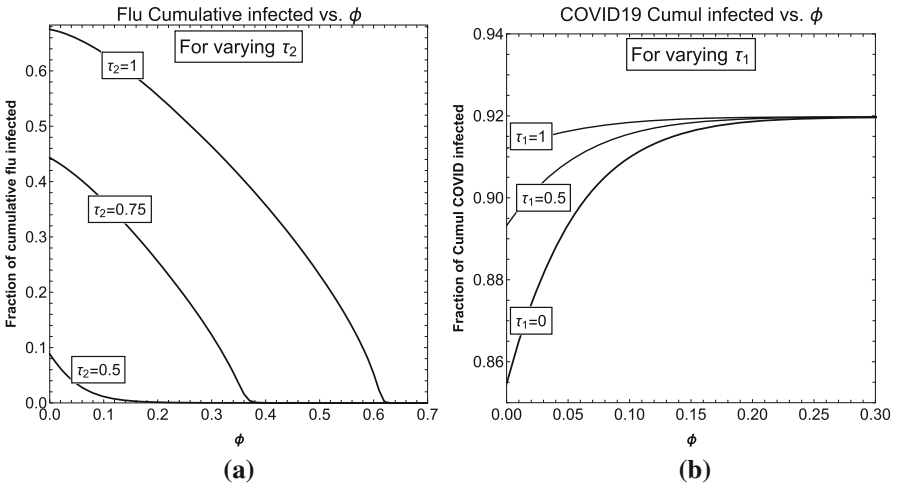

Fig. 3 Cumulative infected of disease 1 (disease 2) vs. ϕ with different amount of τ_2 (τ_1)

increases with τ_1 and ϕ, except if τ_1 is close to one. $\tilde{\mathcal{R}}_2$ increases with ϕ can be interpreted as the more individuals who have received the influenza vaccine results to the more of them are available for infection with COVID-19. However, the closer ϕ to making $\mathcal{R}_1 = 1$, the fewer individuals are infected with influenza. Therefore, the ability of virus interference to affect COVID-19 transmission is irrelevant at the top of Fig. 2(b). τ_1 describes an altered characteristic of individuals who recovered from influenza; however, if ϕ is high enough, there are no individuals infected with influenza ($\mathcal{R}_1 < 1$). Therefore, τ_1 is pointless for high values of ϕ.

Figure 3(a) (Fig. 3(b)) indicates the cumulative proportion of infected with influenza (COVID-19) after 365 days of introducing one infected case with varying ϕ between zero and one, and with different values of τ_2 (τ_1). For Fig. 3(a), we noticed that high values of ϕ indicate that $\mathcal{R}_1 < 1$ and virus interference (τ_2) is irrelevant since the influenza is not going to spread, which is consistent with Fig. 2(a). Further, for lower values of ϕ, τ_2 plays a significant role in reducing the cumulative proportion of infected since by preventing individuals who have had COVID-19 and recovered from getting influenza, that is also preventing them from infecting other individuals. For Fig. 3(b), we observed that as $\phi > 0.2$, τ_1 is irrelevant whereas if no one gets vaccinated ($\phi = 0$), then natural virus interference makes about 5% difference.

We provide numerical simulations of the combined disease burden with varying amounts of influenza vaccine proportion (ϕ) and virus interference factors (τ_1 and τ_2). Figure 4(a) indicates how variations in virus interference factors (τ_1 and τ_2) affect the combined disease burden characteristics when the amount of influenza vaccine proportion (ϕ) varies. The horizontal axis is virus interference by influenza against COVID-19 (τ_1). The vertical axis is virus interference by COVID-19 against influenza (τ_2). Figure 4(a) is created by incrementing τ_2 along the vertical axis, and then for each value of τ_2 increasing τ_1 along the horizontal axis until the threshold characteristic is observed. The first threshold, between region I and II, is whether the disease burden exceeds the asymptotic line, i.e., the first point where the non-monotone increase

occurs. The second threshold is between region II and III, where the combined disease burden at $\phi = 0$ exceeds the asymptotic line for $\phi > 0.6$.

Increasing ϕ from 0 to around 0.2 increases overall COVID-19 incidence due to reduced virus interference; this increases the overall disease burden. At the same time, influenza incidence is decreasing due to vaccination, but the decrease in overall disease burden is outweighed by the increase in COVID-19 until the point where COVID-19 incidence plateaus. After that, flu incidence decreases (as ϕ increases) until it drops to zero as $\mathcal{R}_1$ reaches 1. In region I, this occurs before COVID-19 incidence plateaus, but in regions II and III there is a drop in overall disease burden after COVID-19 incidence plateaus. For virus interference factors (τ_1 and τ_2) in region I, increasing ϕ always raises the combined disease burden (see the solid curve in Fig. 4(b)). For τ_1 and τ_2 in region II, increasing ϕ increases the combined disease burden until the point where the cumulative number of COVID-19 infections stops rising, then combined disease burden decreases until it reaches the asymptotic level, which is the point where the cumulative number of influenza infections is zero. However, in this region, influenza vaccination always increases the combined disease burden relative to vaccinating no one (see the dashed curve in Fig. 4(b)). For τ_1 and τ_2 in region III, increasing ϕ will share the same characteristics as in region II. Still, vaccinating two-thirds or more of the population decreases the combined disease burden relative to vaccinating no one (see the dash-dotted curve in Fig. 4(b)).

Another way to illustrate the net virus interference is by a mathematical description

$$r = \sqrt{(1-\tau_1)^2 + (1-\tau_2)^2},$$

where r is a measure of the net virus interference. (It is the Euclidean distance from (τ_1, τ_2)=(1,1), the top right corner of Fig. 4(a), which represents no virus interference.) Therefore, very roughly, region III is the region when $r < 0.35$, which can be described as low net virus interference. Region II has $r > 0.35$ but $\tau_2 > 0.6$, which can be

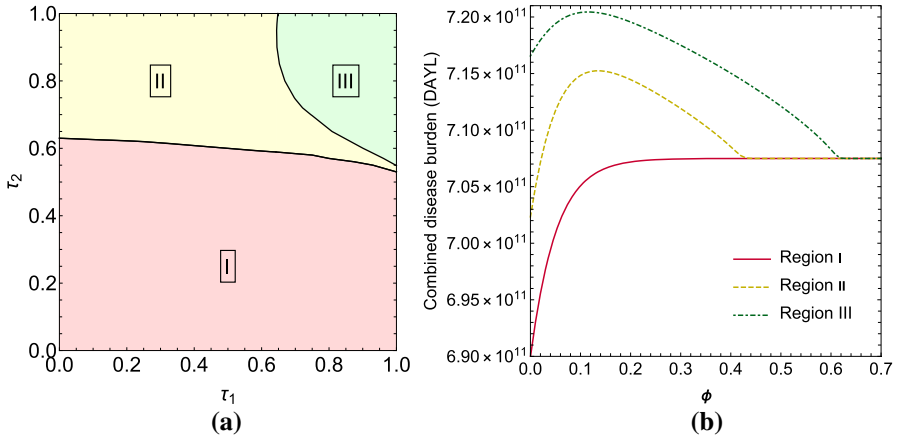

Fig. 4 **a** Variations of virus interference factors (τ_1 and τ_2) against the combined disease burden; **b** The combined disease burden vs. ϕ) with varying amounts of τ_1 and τ_2

explained as significant net virus interference but limited COVID-19-on-influenza interference. Finally, region I has $\tau_2 < 0.6$, which can be described as high COVID-19-on-influenza interference.

5 Discussion and conclusions

Mathematical models help forecast disease dynamics and estimate significant quantities such as disease burden that can be incorporated to evaluate disease control measures such as vaccination. One of the advantages of studies like ours is that it can be carried out early in an outbreak to illustrate the impact of individual factors, before extensive time-series data are available. This study analyzed deterministic models to investigate whether the influenza vaccine increases the combined disease burden of influenza and COVID-19 in a dual outbreak due to a virus interference phenomenon that reduces susceptibility to secondary infections in those who recover from natural primary infections (rather than being vaccinated). The control reproductive numbers $\mathcal{R}_1$ and $\mathcal{R}_1$ as well as the invasion reproductive numbers $\tilde{\mathcal{R}}_1$ and $\tilde{\mathcal{R}}_2$ were computed in this study. Together, these quantities measure a disease's ability to spread in a completely susceptible population or to invade while another disease is present and at equilibrium.

According to this study, the combined disease burden's behavior depends on virus interference factors (τ_1 and τ_2), representing reduced susceptibility, and on the proportion of the population vaccinated against influenza (ϕ). Regardless of virus interference levels, vaccinating two-thirds or more of the population against influenza eliminates the flu outbreak ($\mathcal{R}_1 < 1$). In this case, the cumulative number of influenza infections drops off, and the cumulative number of COVID-19 infections levels off in ϕ, so that for vaccine coverage ϕ of 60% or more, there is effectively no change in the combined disease burden as virus interference levels vary (see Fig. 4(b)). However, virus interference still plays a strategic role, as it affects disease burden at lower vaccine coverage levels, and thus affects whether the combined disease burden is lower for high or low coverage. Depending on the degree of virus interference, the combined disease burden either increases monotonically in ϕ, or rises and then falls to an asymptotic level. As seen in Fig. 4(b), these effects divide virus interference levels into three regions.

If τ_1 and τ_2 fall in region I, indicating that for all values of τ_1 virus interference by COVID-19 (τ_2) gives a 40% or more protection against influenza, then the influenza vaccine is always unhelpful, and the lowest value of the combined disease burden is when no one has received the flu vaccine ($\phi = 0$). In this region (region I), the combined disease burden only increases when the vaccine coverage (ϕ) is between 0% and 20% since, in this interval, the cumulative number of COVID-19 infections increases and the cumulative number of flu infections dies out. Further, when the vaccine coverage (ϕ) is more than 20%, there is no change in the combined disease burden due to no changes in the cumulative number of flu and COVID-19 infections (see the solid curve in Fig. 4(b)).

If τ_1 and τ_2 fall in region II, indicating that virus interference by the flu gives at least 30% protection against COVID-19 and virus interference by COVID-19 gives at most 40% protection against the flu, then influenza vaccine is not beneficial since

the combined disease burden is lower for no vaccine coverage $\phi = 0$ than for vaccine coverage ϕ of 60%. Under this condition, the combined disease burden's lowest value is when $\phi = 0$. In this region, the combined disease burden increases with ϕ when vaccine coverage (ϕ) is between 0% and 20% since the cumulative number of COVID-19 infections increases at a much larger scale than the cumulative number of flu infections decreases. Further, when vaccine coverage (ϕ) is between 20% and 60%, the combined disease burden falls approaching the asymptotic level since the cumulative number of flu infections decreases and no changes in the cumulative number of COVID-19 infections. However, the end results in this region are that vaccinating no one is better than vaccinating two-thirds of the population (see the dashed curve in Fig. 4(b)).

For low net virus interference (region III), influenza vaccination is only beneficial if two-thirds of the population or more have received the influenza vaccine ($\phi > 0.6$) because the combined disease burden is lower for vaccine coverage ϕ of 60% or more than for no vaccine coverage $\phi = 0$. Under this condition, the combined disease burden shares the same qualitative trends as in region II, but the lowest value is when $\phi \geq 0.6$ (see the dash-dotted curve in Fig. 4(b)).

In general, influenza vaccination only lowers the overall disease burden when net virus interference is relatively low (region III) and vaccine coverage is high enough that the reduction in influenza cases more than compensates for any increase in COVID-19 cases. Influenza vaccination may increase the overall disease burden because the average disease burden for one case of COVID-19 is significantly higher than the average disease burden for one case of influenza. Additionally, the actual degree of virus interference in each direction remains a source of some debate, and further studies are needed to measure these factors. However, according to (Wolff 2020), influenza-on-COVID-19 interference (τ_1) is 0.64, which places us either in region I or region II, depending on what COVID-19-on-influenza interference (τ_2) is. Regardless of COVID-19-on-influenza interference (τ_2), the combined disease burden is always higher relatively when vaccinating two-thirds or more of the population.

In cases where two co-circulating diseases have separate burdens and case fatality ratios, vaccinating only a few individuals against one of the diseases may make the other disease increase the combined disease burden more than the vaccine reduces it due to virus interference being a part of the cause. It is essential to get a proper amount of vaccine coverage to overcome the range of increasing overall disease burden. The model structure that we developed could also be used to evaluate the risk of vaccination increasing disease burden by preventing virus interference for other diseases. Hence, it would be important to develop estimates for the degree to which the respective infections interfere with each other by stimulating the body's nonspecific immune response.

The sustained drop in influenza cases during the COVID-19 pandemic is attributed largely to behavior changes (preventive measures) aimed at containing COVID-19 but impacting the spread of most respiratory infections. Behavior changes are another significant factor to take into account (see Alharbi and Kribs 2022), independent of viral interference. Such factors interact and may interfere, as clearly occurs with these two.

One of the limitations of this study is that the actual degree of virus interference is still being debated. As all the epidemiological parameters in the study become better

known, we will have not just a better idea of where the region boundaries are, but a better idea of which region we are in. In the future, a study can be extended to consider vaccination in both diseases since vaccinating the world's population against COVID-19 is currently a primary focus of world public health. Only when a large proportion of the population has been vaccinated will we begin to observe effects such as those outlined in this study.

A long enough epidemic–certainly including the present COVID-19 epidemic–changes certain transmission elements. Vaccine efficacy may wane over time, especially as new variants emerge, and since virus interference occurs when two infections take place within the time frame of the body's nonspecific immune response, those who recover from either disease will eventually pass into a state where any viral interference is greatly diminished, as that nonspecific immune response winds down. This partially mitigates the overall effect of viral interference. COVID-19 vaccination, not incorporated in the original model, also further affects susceptibility to infection.

References

Alharbi MH, Kribs CM (2022) How the nature of behavior change affects the impact of asymptomatic coronavirus transmission. Ricerche di Matematica, pp 1–21

Alharbi MH, Kribs CM (2021) A mathematical modeling study: assessing impact of mismatch between influenza vaccine strains and circulating strains in hajj. Bull Math Biol 83(1):1–26

Amato M, Werba JP, Frigerio B, Coggi D, Sansaro D, Ravani A, Ferrante P, Veglia F, Tremoli E, Baldassarre D (2020) Relationship between influenza vaccination coverage rate and COVID-19 outbreak: an Italian ecological study. Vaccines 8(3):535

CDC (2020) Estimated influenza illnesses, medical visits, hospitalizations, and deaths in the United States - 2019-2020 Influenza Season. https://www.cdc.gov/flu/about/burden/2019-2020.html#flu-burden-infographic. Accessed: March 2021

CDC (2021) Demographic Trends of COVID-19 cases and deaths in the US reported to CDC. https://covid.cdc.gov/covid-data-tracker/#demographics. Accessed: March 2021

Cowling B, Nishiura H (2012) Virus interference and estimates of influenza vaccine effectiveness from test-negative studies. Epidemiology 23(6):930–931

Cowling BJ, Fang VJ, Nishiura H, Chan K-H, Ng S, Ip DKM, Chiu SS, Leung GM, Peiris JSM (2012) Increased risk of noninfluenza respiratory virus infections associated with receipt of inactivated influenza vaccine. Clin Infect Dis 54(12):1778–1783

Ding Q, Panpan L, Fan Y, Xia Y, Liu M (2020) The clinical characteristics of pneumonia patients coinfected with 2019 novel coronavirus and influenza virus in Wuhan. China. J Med Virol 92(9):1549–1555

EBMPHET Consortium (2020) COVID-19 severity in Europe and the USA: Could the seasonal influenza vaccination play a role? Soc Sci Res Netw. https://doi.org/10.2139/ssrn.3621446

Feng S, Fowlkes AL, Steffens A, Finelli L, Cowling BJ (2017) Assessment of virus interference in a test-negative study of influenza vaccine effectiveness. Epidemiology 28(4):514

Kelly H, Barry S, Laurie K, Mercer G (2010) Seasonal influenza vaccination and the risk of infection with pandemic influenza a possible illustration of non-specific temporary immunity following infection. Eurosurveillance 15(47):19722

Kribs-Zaleta CM, Mubayi A (2012) The role of adaptations in two-strain competition for sylvatic trypanosoma cruzi transmission. J Biol Dyn 6(2):813–835

Lisewski AM (2020) Association between Influenza Vaccination Rates and SARS-CoV-2 Outbreak Infection Rates in OECD Countries. Soc Sci Res Netw. https://doi.org/10.2139/ssrn.3558270

Martínez-Baz I, Trobajo-Sanmartín C, Arregui I, Navascués A, Adelantado M, Indurain J, Fresán U, Ezpeleta C, Castilla J (2020) Influenza Vaccination and risk of SARS-CoV-2 infection in a cohort of health workers. Vaccines 8(4):611

Merler S, Poletti P, Ajelli M, Caprile B, Manfredi P (2008) Coinfection can trigger multiple pandemic waves. J Theor Biol 254(2):499–507

Mitchell C, Kribs C (2019) Invasion reproductive numbers for periodic epidemic models. Infect Dis Model 4:124–141

Murray CJ (1994) Quantifying the burden of disease: the technical basis for disability-adjusted life years. Bull World Health Organ 72(3):429

Opatowski L, Baguelin M, Eggo RM (2018) Influenza interaction with cocirculating pathogens and its impact on surveillance, pathogenesis, and epidemic profile: a key role for mathematical modelling. PLoS Pathog 14(2):e1006770

Ozaras R, Cirpin R, Duran A, Duman H, Arslan O, Bakcan Y, Kaya M, Mutlu H, Isayeva L, Kebanlı F et al (2020) Influenza and COVID-19 Co-infection: report of 6 cases and review of the literature. J Med Virol 92(11):2657–2665

Porco TC, Blower SM (1998) Designing hiv vaccination policies: subtypes and cross-immunity. Interfaces 28(3):167–190

Shahid Z, Kalayanamitra R, McClafferty B, Kepko D, Ramgobin D, Patel R, Aggarwal CS, Vunnam R, Sahu N, Bhatt D et al (2020) COVID-19 and older adults: what we know. J Am Geriatr Soc 68(5):926–929

Suzuki M, Camacho A, Ariyoshi K (2014) Potential effect of virus interference on influenza vaccine effectiveness estimates in test-negative designs. Epidemiol Inf 142(12):2642–2646

U.S. Census Bureau (2019). Annual Estimates of the resident population for selected age groups by sex for the United States: April 1, 2010 to July 1, 2019. https://www.census.gov/newsroom/press-kits/2020/population-estimates-detailed.html, 2019. Accessed: March 2021

Van den Driessche P, Watmough J (2002) Reproduction numbers and sub-threshold endemic equilibria for compartmental models of disease transmission. Math Biosci 180(1–2):29–48

Van Beek J, Veenhoven RH, Bruin JP, Van Boxtel RAJ, De Lange MMA, Meijer A, Sanders EAM, Rots NY, Luytjes W (2017) Influenza-like illness incidence is not reduced by influenza vaccination in a cohort of older adults, despite effectively reducing laboratory-confirmed influenza virus infections. J Infect Dis 216(4):415–424

Velasco-Hernández JX, Núñez-López M, Comas-García A, Cherpitel DEN, Ocampo MC (2015) Superinfection between influenza and RSV alternating patterns in San Luis Potosí State. México. PloS One 10(3):e0115674

Wolff GG (2020) Influenza vaccination and respiratory virus interference among department of defense personnel during the 2017–2018 influenza season. Vaccine 38(2):350–354

Zhang P, Sandland GJ, Feng Z, Xu D, Minchella DJ (2007) Evolutionary implications for interactions between multiple strains of host and parasite. J Theor Biol 248(2):225–240